ELSEVIER

Contents lists available at ScienceDirect

# Reliability Engineering and System Safety

journal homepage: www.elsevier.com/locate/ress





# Flood fragility assessment of bridges—Unified framework

Athanasia K. Kazantzi <sup>a,\*</sup> , Konstantinos Bakalis <sup>b</sup> , Stergios-Aristoteles Mitoulis <sup>c</sup>

- a Department of Civil Engineering, International Hellenic University, Serres, Greece
- <sup>b</sup> School of Civil Engineering, National Technical University of Athens, Athens, Greece
- <sup>c</sup> Department of Civil Engineering, School of Engineering, University of Birmingham, Birmingham, UK

#### ARTICLE INFO

Keywords:
Unified method
Bridge
Flood fragility
Pier
Scour
Incremental flood analysis
Vector intensity measure

#### ABSTRACT

This paper provides an analytical step-by-step probabilistic framework for undertaking a flood fragility assessment of bridges considering a spectrum of foundation scour severity scenarios. Currently, and despite the fact that bridge fragilities to natural hazards (e.g., earthquakes) are at a relatively mature stage-constituting the state-of-the-art in undertaking pertinent risk assessment studies-bridge flood fragilities and the relevant methodologies are scarce in the literature. This knowledge gap prevents us from delivering either quantitative flood risk assessments for existing bridge portfolios or risk-aware flood performance evaluations for new bridge designs. To address this gap, this paper proposes, for the first time, a unified probabilistic framework, that is showcased for a typical road bridge with piers on shallow foundations, which is not bridge-specific. The framework is applicable, with appropriate adjustments, to other bridge components and typologies. By means of numerical simulations on reduced-order Monte Carlo generated bridge pier samples, the response statistics of the considered bridge pier are being evaluated at increasing flood intensity levels through incremental flood-relevant static analyses by applying equivalent hydrodynamic forces. The flood intensity accounts for both the flow velocity and inundation depth, based on a new vector intensity measure. Different sets of flood fragility curves are produced for variable scour severity scenarios, whereas intra-scour severity scenario randomness is captured by considering a spectrum of plausible scour patterns. It is demonstrated that scour has a detrimental impact on the flood fragility of bridges, whereas if minimised by taking appropriate proactive measures, the probability of the bridge being severely damaged becomes very low even under the most severe realistic flood intensities. The proposed framework could serve a first-order flood risk assessment tool for large bridge inventories, offering to engineers, asset managers and network operators quantitative means for resource allocation and the implementation of adaptation measures.

#### 1. Introduction

Floods and subsequent adverse hydraulic stressors on bridges, e.g., scour and debris accumulation, constitute common mechanisms triggering bridge failure [1]. In the United States, approximately 60 % of all recorded bridge failures have been associated with hydraulic actions [2] while in the United Kingdom, the annual cost for bridge maintenance and repairs amounts to £180 m [3]. In the EU, Slovenia witnessed the most devastating floods ever recorded in the country in August 2023. Roads, bridges and houses were swept away and severely impacted [4]. The region of Thessaly, Greece, was also recently severely affected by floods [5,6]. Storm Daniel caused the worst flash floods ever recorded in the country, leaving 79 bridges damaged out of which 24 need to be completely rebuilt [7], creating an extremely challenging and puzzling

predicament for infrastructure decision-makers. Interestingly, the same region and its infrastructure were repeatedly and severely affected in 2016 and 2020 [8] by strong Mediterranean hurricanes (Medicanes) [9], showcasing the repetitive nature of extreme flood incidents, as well as the high likelihood of an asset being adversely affected more than once throughout its lifetime. In all these cases, partial or global collapses due to flooding were witnessed not only in old bridges, but also in bridges that have not yet exceeded their design lifetime. Based on these recent events, the timeframe between successive extreme incidents could be narrow thus not allowing adequate assessment and design time for applying any appropriate reactive interventions.

The ever-increasing frequency and intensity of extreme events [10] (i.e., floods [11]) come as a direct result of climate impacts, affecting modern transport infrastructure, with severe consequences cascading

<sup>\*</sup> Corresponding author at: Department of Civil Engineering, International Hellenic University, 62124, Serres, Greece. *E-mail address:* kazantzi@ihu.gr (A.K. Kazantzi).

into transport and other interdependent networks [12–14]. It is predicted that approximately 20 % of the bridge stock will require protection against scour (e.g., rip-rap or rock rolls [15]) in the next decades due to increased river floods [16]. With the cost of providing scour mitigation protection in bridges amounting to only 5 % of the total construction cost [17], proactive measures are substantially less costly than reactive ones. On account of the above, it is necessary to develop practical methods that will enable the assessment of flood performance/vulnerability of stream-crossing bridges and their components. In particular, the engineering community currently lacks the proper tools to enable either flood risk-informed design decisions or proactive countermeasures, in view of enhancing flood resilience. This is a well acknowledged gap in the international literature.

A key element of the risk assessment, mitigation and investmentprioritisation activities for infrastructure assets such as bridges, are the so-called fragility curves, i.e., the conditional probability of exceeding performance/capacity criteria under certain natural hazard stressors. While research efforts are geared towards the assessment of bridges under a single-[18,19] or a multi-hazard context [20-25], very few studies exist in the international literature that explicitly focus on the flood fragility of bridges [26–28]. Moreover, even the few existing ones are mainly focused on bridge-specific applications and often employ detailed finite element bridge models (e.g., [28-31]) that are not suitable for large-scale bridge portfolio assessments [32]. Also, flood fragilities for bridge classes [33,34], with the bridges within the same class sharing a common set of influential flood performance characteristics (e.g., material, era of construction, foundation type etc), do not currently exist in the literature, despite the fact that this approach is relatively popular in large asset portfolio assessments that account for other natural hazards (e.g., earthquakes, see for instance [35,36]) and engineering structures [34,37,38].

One of the few bridge flood fragility models that are available in the literature, is the Hazus flood model [39]. This model provides empirical failure probability estimates considering the return period of the flood, the extent of scour and the typology of the bridge span (i.e., single or continuous). However, this model is not extensively calibrated whereas it is also built solely upon the US National Bridge Inventory for obtaining the failure probability estimates. Therefore, significant adaptation is required to extend its applicability in other countries that follow different construction methods. Another recent attempt by Loli et al. [8] towards assessing the flood bridge vulnerability, involved a qualitative indicator-based framework to capture the propensity of river-crossing bridges to flood-induced damages. Yet, although useful for undertaking a risk-aware preliminary prioritisation of mitigation actions, the methodology is not suitable for quantitative flood hazard assessment procedures.

An additional flood resilience assessment study is that of Khandel and Soliman [19]. This research proposes a probabilistic framework for assessing the flood fragility of bridges via deep learning neural networks. Hence, to enable the computation of flood fragility estimates as a function of service life and river discharge, a training set needs to first be generated for implementing the proposed method. This requires a non-trivial effort, that is not justified for a framework that is bridge and location specific. A more simplified, yet more generic approach, is offered by Arora and Benerjee [40]. The proposed method requires the development of performance functions for capturing the most probable failure modes. Then it adopts the First Order Reliability Method (FORM) to estimate the bridge failure probabilities. Although this method requires substantially less resources compared to those that are founded upon numerical simulations, it carries all the limitations of the FORM approach, which is mainly related to the inaccuracies in the cases of highly nonlinear problems.

Therefore, there is an emerging need for developing a practical quantitative bridge flood response and fragility assessment methodology to enable the performance-based flood design and assessment of bridges and consequently risk-informed decision-making [41]. This paper

proposes a new *unified* framework to accomplish the aforementioned goal. This is done through developing representative numerical models of the main bridge components, to allow for the consideration of several influential random parameters that are likely to affect the flood performance of the bridge asset under investigation. The numerical probabilistic framework that is proposed, suits well the needs of both assetand class-specific fragility assessment studies. The fragility methodology is demonstrated herein for reduced-order bridge pier models so as to remain practical even when it is utilised for class fragility assessment studies. The reduced-order models are subjected to incrementally scaled hydraulic forces considering response variations due to the randomness of the bridge-soil system properties, the applied traffic loads and the impact of the scour at the foundation.

# 2. Framework for the response assessment of bridge piers to floods

The flowchart of the proposed framework for undertaking a flood response and fragility assessment of bridge piers is illustrated in Fig. 1. The methodology involves five distinct steps: (a) definition of the bridge pier of interest, i.e., typology, geometry, applied loads and soil properties, (b) establishment of plausible scour patterns, each one associated with a specific scour severity scenario (e.g., low, moderate, extensive and severe), (c) identification and treatment of uncertainty sources that may have an impact on the expected bridge pier response, (d) development of a representative reduced-order finite element model and Monte Carlo simulations for generating the bridge pier samples to account for the uncertainties that come into play and (e) evaluation of the bridge pier flood response statistics having subjected each scoured bridge pier sample (associated with certain scour severity scenarios) to incrementally scaled flood induced hydraulic forces, i.e., to different flood height levels (i.e., inundation depths) and incrementally scaled flood velocities. The aforementioned methodology could be extended to other bridge components and typologies with appropriate adjustments. Yet, in the following sections the focus will be on shallow foundation bridge piers with simple supported decks. This is a reasonable and representative assumption for existing river-crossing bridges and facilitates the way the steps involved in the proposed methodology are presented.

## 3. Modelling aspects

## 3.1. Bridge pier modelling

In view of the complexity of the problem at hand as well as the number of analyses required, a reduced-order modelling approach is adopted to generate the response statistics of the bridge component of interest, that, as mentioned above, will be a bridge pier on shallow foundation. Both the bridge pier and its pad footing are typically modelled utilising elastic beam-column elements [42]. The reason behind this assumption is that, under the flood induced hydraulic forces, limited material nonlinearity is anticipated to be developed in the pier-foundation structural elements for the drift levels of interest (i.e., < 1% [21]). This simplification essentially implies that the piers and their spread foundations have sufficient strength and stiffness to resist the hydraulic forces without developing any substantial material nonlinearity prior to the occurrence of the dominant failure mechanism. The latter is herein associated with a certain tilting level for the piers (e.g., [43,44]) under both flood-induced horizontal forces and potential local scour conditions. The elastic beam-column elements utilised for modelling the pier and the spread footing are readily available in the element library of the OpenSees software platform [45,46] that was employed for computing the flood induced demands on the pier. For the case at hand, the bridge pier beam-column elements were assigned their actual stiffness, whereas those utilised for modelling the strip footing were assumed to be rigid. Furthermore, P- $\Delta$  effects, i.e. global geometric

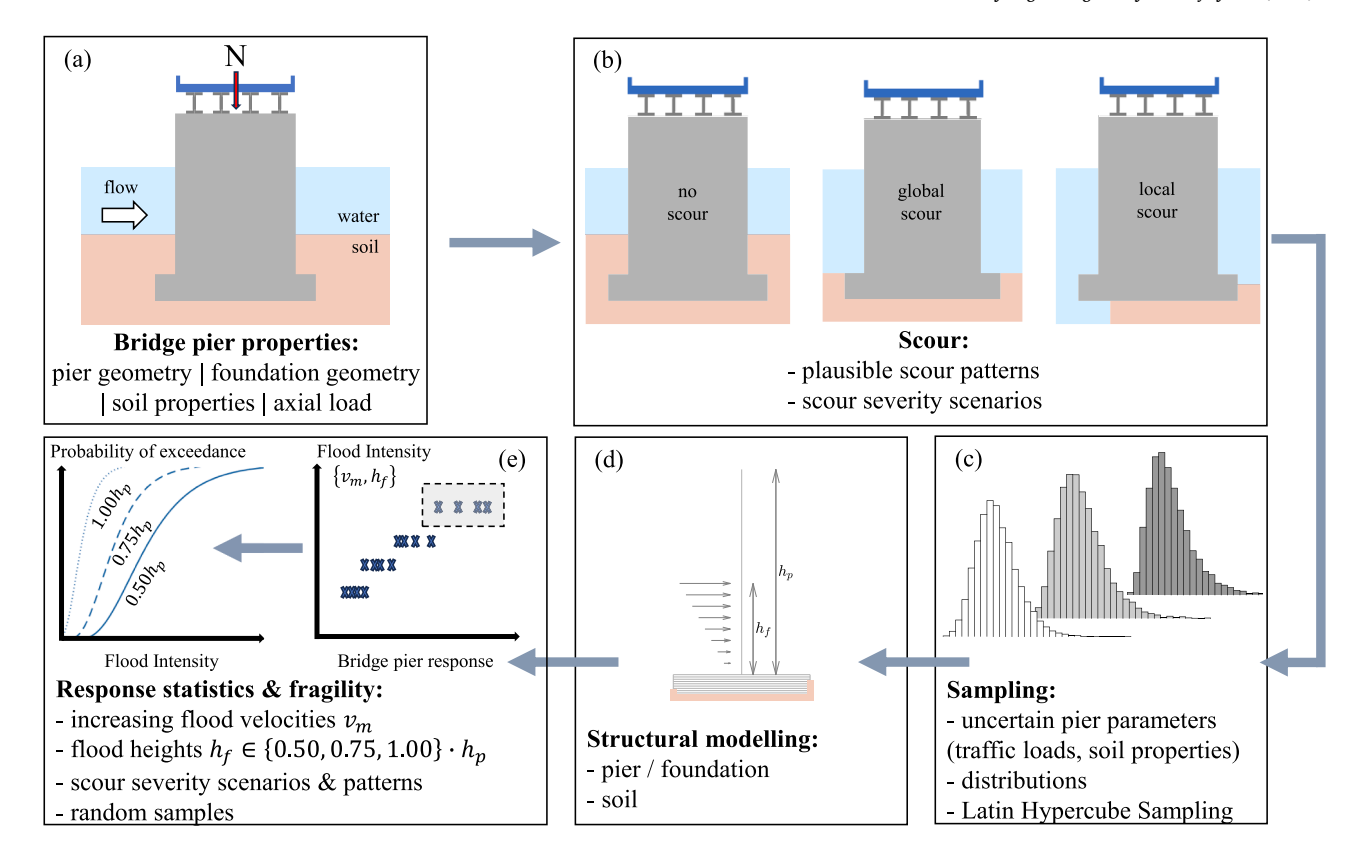
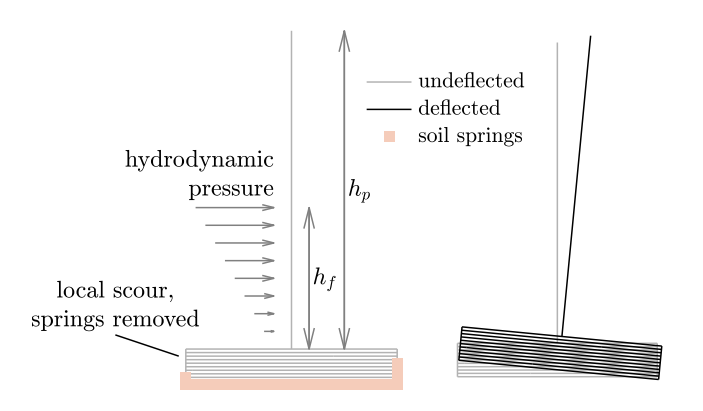


Fig. 1. Flowchart of the proposed methodology, featuring the generation of flood fragility curves of a bridge pier with shallow foundation.

nonlinearities, were taken into account. A schematic representation of the bridge pier model and the surrounding soil springs is illustrated in Fig. 2.

#### 3.2. Soil modelling

To model the interaction between the pier spread footing and the surrounding soil, a series of horizontal and vertical elastic no-tension (ENT) springs were utilised (e.g., [42,47]). The stiffness of those springs was evaluated based on the expressions proposed by Gazetas [48] for shallow bearing footings, that are assumed to be rigid compared to the surrounding soil. The expressions provide estimates for the stiffness of the foundation (impedances) as a function of the footing geometry, the depth of the foundation (d) as well as the shear modulus ( $G_s$ )



**Fig. 2.** Reduced-order model of the bridge pier showing its original position and the deformed shape under the flood hydraulic forces for the case of a shallow foundation bridge pier foundation with upstream and downstream local scour; local scour is taken into account by removing soil springs from the foundation.

and the Poisson's ratio  $(v_s)$  of the soil [49]. The impedances, evaluated according to the expressions proposed by Gazetas [48] along the vertical  $(k_z)$  and the horizontal  $(k_x)$  direction of the strip footing, were uniformly distributed in the springs that are located across the length of the foundation sides as illustrated in Fig. 3. The rotational stiffness of the foundation is implicitly accounted for through the differential movement of the vertical springs. It should be noted that the uncertainties associated with the definition of the spring coefficients are large and could have a notable impact on bridge engineering design and assessment projects [50]. For instance, as reported by Faraonis et al. [51], the shear modulus of soil could be overestimated by approximately 20 % even in controlled laboratory conditions.

#### 3.3. Scour modelling

Of particular interest to the flood performance of bridge piers is the

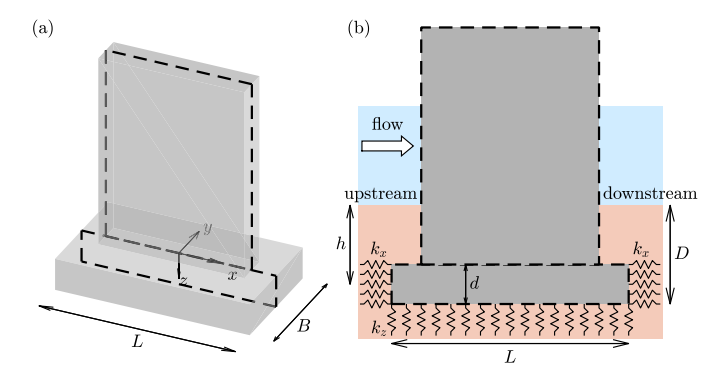


**Fig. 3.** Soil-Structure-Interaction modelling approach of a shallow foundation bridge pier: (a) three-dimensional view of the bridge pier; (b) two-dimensional view of the bridge pier featuring the soil impedances considered.

modelling of the scour. It is considered a major underlying cause that has the potential to trigger pier foundation failure and destabilisation under extensive translational and rotational movement, or even failure of the deck in certain cases (e.g., [52-55]). Scour is classified into two main categories, i.e., global and local scour (e.g., [36]). Global scour occurs due to the ongoing erosion of the riverbed soil. By contrast, local scour occurs in the vicinity of the bridge piers or abutments as a consequence of the flow disruption due to the presence of structural elements within the river channel. Both the extent and the scour hole geometry around the bridge pier are highly uncertain factors [56]. Furthermore, the evolution of scour over the lifetime of a bridge is also highly uncertain and its proper consideration requires probabilistic treatment [57-61]. In fact, scour could occur and evolve under both normal and flood flow conditions [62]. In this study, the exact process of the scour evolution and development mechanism over time is not explicitly modelled. Instead, flood performance of bridge piers is evaluated under certain scour depths and patterns on their foundation, disregarding whether this refers to past scour (subject to the condition of "zero" visible tilting prior to the occurrence of the flood), a scour that was developed during a considered flood event, or more likely both. This approach is essentially a cause-agnostic [63] scour treatment, in the sense that one is not interested in its progression over time, but mainly in the scour condition of the bridge pier when the latter is subjected to the maximum hydraulic force during an extreme flood occurrence. Hence, herein we have assumed flood intensity and scour being uncorrelated. This assumption

implies that the extent of scour is not necessarily associated to one single flood event. This way, historical scour induced damages can be considered.

Different scour scenarios are investigated herein for the considered shallow foundation bridge pier typology. The effect of local scour in the developed bridge pier model was accounted for by removing soil springs from the foundation (e.g., [64]). Any scour that occurs above the top level of the footing is assumed to be the result of global scour in this study. The occurrence of global scour affects the impendences that are evaluated for the soil springs, as shown in Table 1. The parametric study that was conducted with regard to the scour depth and pattern accounts for both uniform global scour around the foundation (see top and mid rows in Table 1) as well as local scour patterns presented in the bottom row of Table 1, in Table 2 and indicatively in Fig. 4. In Table 1,  $z_{su}$  and  $z_{sd}$ are the (vertical) scour distances upstream and downstream, respectively. For local scour scenarios, scour severity (i.e., depth) is considered higher (or equal) on the upstream side compared to that developed on the downstream side [65]. Side upstream or downstream local scour is expressed as a percentage of the soil height that is removed from the side of the shallow foundation footing, measured from the top level of the footing (Table 1). Hence, 0 % upstream scour i.e., no upstream local side-scour, means that the soil is still up to the top level of the footing in the upstream side whereas maximum global scour depth (i.e., up to the top level of the footing) has been developed (Table 1). In fact, all local scour scenarios are developed assuming that maximum global scour (i.

**Table 1**Scour scenarios and soil spring impedances for a shallow foundation bridge pier (the red dashed line corresponds to the upper level of the unscoured foundation depth).

Scenarios	Graphical representation	Evaluation of impedances
Uniform global scour: $z_{su} = z_{sd}$ $z_{su} < D - d$ and $z_{sd} < D - d$	upstream downstream $k_x$ $L$	Evaluate $k_x$ and $k_z$ for $z_s \in (0, D-d)$
Uniform global scour: $z_{su}=z_{sd}$ $z_{su}=D-d$ and $z_{sd}=D-d$	$z_{su} \downarrow h \qquad downstream \\ k_x \qquad k_x \\ L$	Evaluate $k_x$ and $k_z$ for $z_s = D - d$
(Non-) uniform local scour: $z_{su} \geq z_{sd}$ $z_{su} > D-d$ and $z_{sd} \geq D-d$	$z_{su}$ downstream $k_x$ $D$ $k_z$ $k_z$ $k_z$ $k_z$ $k_z$ $k_z$	Evaluate $k_x$ and $k_z$ for $z_{\rm s}=D-d$ and remove soils springs accordingly (see also Table 2 and Fig. 4)

**Table 2** Global (1) and local (2-19) scour patterns.

	· · ·		
Case ID	Upstream	Downstream	Under-scour (Upstream)
0*	N/A	N/A	N/A
1**	0 %	0 %	0 %
2	20 %	20 %	0 %
3	40 %	40 %	0 %
4	60 %	60 %	0 %
5	80 %	80 %	0 %
6	100 %	0 %	10 %
7	100 %	20 %	10 %
8	100 %	40 %	10 %
9	100 %	60 %	10 %
10	100 %	80 %	10 %
11	100 %	0 %	20 %
12	100 %	20 %	20 %
13	100 %	40 %	20 %
14	100 %	60 %	20 %
15	100 %	80 %	20 %
16	100 %	0 %	30 %
17	100 %	20 %	30 %
18	100 %	40 %	30 %
19	100 %	60 %	30 %

<sup>\*</sup> Case 0 reflects the unscoured case (no global or local scour).

e., scour up to the top level of the foundation) has already been developed.

#### 4. Hydrodynamic forces

The hydrodynamic pressure p that acts on the pier in the direction of the flow, was evaluated in this study according to the provisions of EN1991-1-6 [66]. In EN1991-1-6 [66] the exerted flow pressure on the pier is evaluated by the following equation:

$$p = k \cdot \rho_{wa} \cdot v_m^2 \tag{1}$$

In Eq. (1), k is a shape factor that equals 1.44 for objects of square or rectangular horizontal cross section and 0.70 for those of circular horizontal cross section;  $\rho_{wa}$  is the density of the water in kg/m<sup>3</sup>; and  $\nu_m$  is the mean flood velocity, averaged over the depth in m/s.

The maximum value of the pressure is found at the free surface of the water and its distribution over the water height is approximated with a triangular distribution. Referring to the load application, EN1991-1-6 [66] specifies that the hydrodynamic pressure should solely be applied on the length of the pier that spans from the free water surface to the

general surface of the riverbed, as this is formulated considering only global scour (if any). Fig. 5 illustrates how the hydrodynamic pressure was applied to the pier model variations for different global and local scour scenarios. Assuming a triangular distribution, the total horizontal force may be evaluated as [66]:

$$F_{wa} = \frac{1}{2} \cdot k \cdot \rho_{wa} \cdot \nu_m^2 \cdot h_f \cdot b \tag{2}$$

In Eq. (2),  $h_f$  is the water depth excluding the local scour depth (see also Fig. 5), and b is the width of the pier.

#### 5. Fragility assessment

#### 5.1. Background

Several methods exist in the literature for estimating the fragility of an asset, or a system of assets, against certain or multiple natural hazards, i.e., empirical, analytical, hybrid [67]. Of those methods, the most accurate is the empirical one [67] subject to the sufficient quality and quantity of the available observations [68]. However, its widespread application is mainly hampered by the scarcity of historical data for the assets' portfolio of interest. Due to this limitation, irrespectively of the natural hazard under investigation, analytical fragilities remain a very attractive alternative. For earthquake engineering in particular, such a tool is considered a mainstream approach for the assessment of structural performance, in view of the vast uncertainties involved. By contrast, flood fragilities have received considerably less attention and are substantially less well documented in the international literature. The latter becomes more evident for the case of flood fragilities of bridges [30].

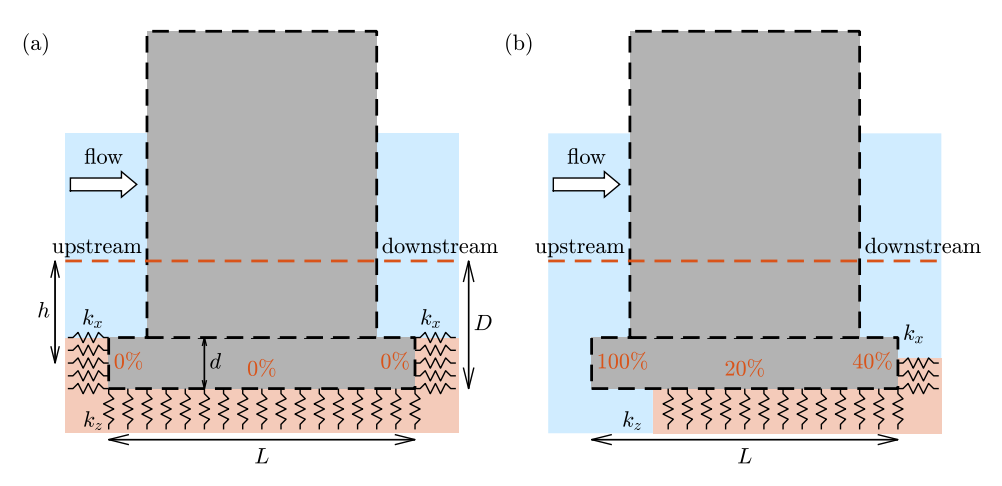
The flood fragility,  $F_{DS}(IM)$  denotes the probability of an EDP demand D, where EDP refers to an appropriate Engineering Demand Parameter, exceeding a certain EDP capacity threshold  $C_{DS}$  paired to a specific damage state, conditioned to an Intensity Measure (IM) level:

$$F_{DS}(IM) = P(D > C_{DS} \mid IM)$$
(3)

Under the typical lognormal assumption [69,70], fragility may be expressed as:

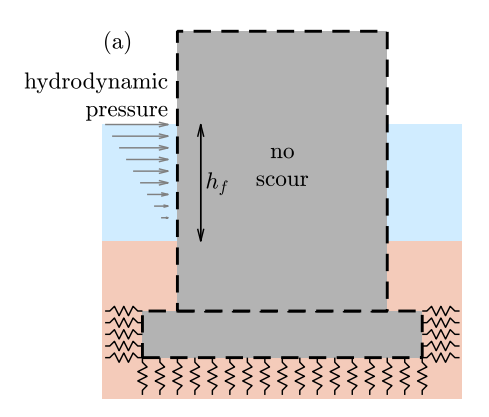
$$F_{DS}(IM) = \Phi\left(\frac{\ln EDP(IM)_{50\%} - \ln EDP_{C,50\%}}{\beta_{tot}}\right)$$
 (4)

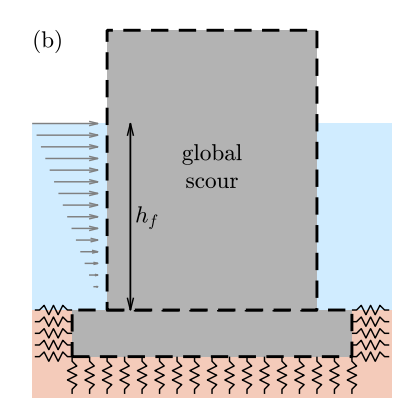
In Eq. (4),  $EDP(IM)_{50\%}$  is the median demand and  $EDP_{C.50\%}$  is the median capacity for every IM level.  $\beta_{tot}$  is the total dispersion (assuming that the dispersion of the demand and the capacity are uncorrelated) evaluated as:



**Fig. 4.** Indicative scour patterns for a shallow foundation pier: (a) global scour of the soil up to the upper level of the foundation with no local scour (Case 1 in Table 2); (b) local scour scenario where 100 %, 40 % and 20 % of the upstream, downstream and under soil are removed, respectively (Case 13 in Table 2); the red dashed line indicates the original level of ground in the unscoured foundation.

<sup>\*\*</sup> Case 1 reflects the maximum considered global scour case with no local scour (Fig. 4a).





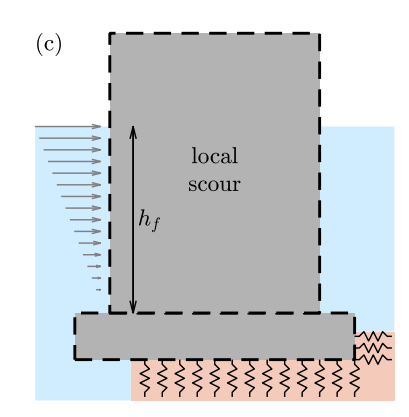


Fig. 5. Distribution of hydrodynamic pressure for (a) the unscoured case, (b) maximum global scour case and (c) local scour case with upstream, downstream and under scour.

$$\beta_{tot} = \sqrt{\beta_{\text{EDP}|M}^2 + \beta_C^2} \tag{5}$$

In Eq. (5),  $\beta_{EDP|IM}$  is the dispersion of the EDP given an *IM* level and  $\beta_c$  is the threshold capacity dispersion.

#### 5.2. Flood intensity measure

To establish a relationship between flood hazard and structural response, an IM is required to characterise the severity of the hydrological phenomenon. Past literature [27,30] suggests that the mean flood velocity  $v_m$  is a relatively representative IM for floods. However, given the particularities of the river geometry at the location of interest, for the same  $v_m$  different water heights  $h_f$  may be encountered. As reported in Ahamed et al. [31], on the basis of a hydraulic analysis for a certain location, the same flood velocity may be associated with different discharge levels whereas the inundation depth steadily increases for higher discharges. In theory, discharge (which is evaluated as a product of the water velocity and the cross-sectional area of the river) can be utilised as an alternative IM [26,31,71], since it uniquely characterises the hydraulic conditions at the location of interest. However, considering that flood velocity and inundation depth are two parameters that are necessary to evaluate the response of the bridge when performing an analytical assessment, the response statistics are evaluated herein on the basis of a vector-valued *IM*, that is defined as  $\{v_m, h_f\}$  [72, 73]. Hence, for each  $v_m$  the response statistics are evaluated for different levels of incrementally scaled  $h_f$ . This process essentially accounts for the fact that the same flood velocity could be associated with different discharge levels and thus different inundation depths. Furthermore, the vector IM yields fragility curves that are not location-specific, a condition that is useful in applications to extract flood fragility curves for bridge classes. This essentially means that the statistics of the responses are evaluated on a location-agnostic basis, and then one could evaluate the probability of the bridge being in or exceeding a certain damage state on account of the fragility that better reflects the relationship between the velocity and inundation depth at the location of interest.

#### 5.3. Engineering demand parameters and damage states

In the context of performance-based assessment of structures, appropriate damage states (DSs) of increasing severity need to be defined. Each DS is associated with the exceedance of capacity thresholds that refer to engineering demand parameters which are deemed to be suitable metrics for assessing the structural response of the bridge. In this study, the titling of the pier was assumed to be a representative EDP for characterising the damage state of the bridge pier. The criteria and thresholds proposed by Mitoulis et al. [74] for pier tilting are used to signify the transition of the bridge from one DS to the other. The thresholds considered herein are summarised in Table 3. Pier tilting

below 0.1 % is associated with the event of 'no damage', whereas exceeding the capacity thresholds of 0.1 %, 0.2 %, 0.4 % and 0.6 %, signifies the transition of the bridge to 'minor', 'moderate', 'extensive' and 'severe' level of damage, respectively. Hence, in case that the response of a bridge pier exceeds for instance the 0.1 % tilting threshold, that signifies that the bridge pier falls in or exceeds DS1.

Bearing in mind that this study aims to present a methodology for flood fragility assessment, it is solely focused on one of the most dominant failure modes, i.e. pier tilting. Deriving the overall bridge fragility simply requires the computation of flood fragility curves for each bridge component in order to obtain the so-called "combined" component fragility curve [75]. The latter denotes the probability of the bridge being at a certain DS given an *IM* level, considering that the bridge DS coincides with the worst DS that is signalled for the bridge due to the damage evaluated across the individual bridge components.

#### 6. Case study

#### 6.1. Benchmark bridge pier

A three-span prestressed concrete bridge with shallow foundations is adopted to demonstrate the methodology presented above. The reason for this choice is that bridges with shallow foundations are very common and are generally expected to be more vulnerable to floods compared to bridges with deep foundations [76]. The case study bridge has a total length of 100.5 m and each one of its two instream piers of rectangular cross section, supports a total bridge span of 33.5 m and a deck with a width of 13.5 m. The deck of the bridge rests on the bridge piers by means of bearings . A generic overview of the baseline bridge is provided in Fig. 6, featuring the pier under investigation. Table 4 summarises the main geometric, load and soil properties of the baseline bridge application. Additional information on the case study bridge is available by Argyroudis and Mitoulis [56]. The developed methodology is applicable to other bridge geometries and typologies, with appropriate adjustments needed in the latter case.

**Table 3**Damage state classification and capacity thresholds for spread foundation bridge piers.

Damage State (DS)	Level of damage	Capacity thresholds
DS0	No damage	Pier tilting < 0.1 %
DS1	Minor	Pier tilting $> 0.1$ %
DS2	Moderate	Pier tilting $> 0.2$ %
DS3	Extensive	Pier tilting > 0.4 %
DS4	Severe	Pier tilting $> 0.6$ %

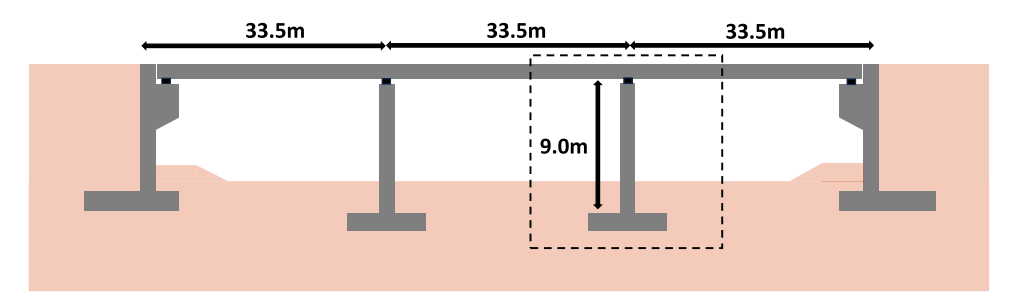


Fig. 6. Side view of the considered shallow foundation benchmark bridge (not to scale).

**Table 4**Properties of the case study pier-foundation system - baseline model.

Property	Notation	Units	Value
Shape factor	k	-	1.44*
Pier height	$h_p$	m	9.00
Pier breadth	$B_p$	m	1.00
Pier length	$L_p$	m	4.50
Depth of footing	ď	m	1.00
Breadth of footing	В	m	3.50
Length of footing**	L	m	6.00
Foundation depth	D	m	2.50
Soil Shear modulus	$G_s$	MPa	50.00
Poisson's ratio	$ u_{sat}$	-	0.35
Deck dead loads	$N_{DL}$	kN	7839.00
Deck live loads	$N_{LL}$	kN	746.00

<sup>\*</sup> object of square or rectangular horizontal cross section.

#### 6.2. Uncertainty consideration

To obtain the flood fragilities, randomness in the following parameters is taken into account at each level of flood intensity: (a) randomness in the shear modulus of the soil  $G_s$ , considering that the footing is founded on a clayed sand soil for the case at hand; (b) randomness in the Poisson's ratio for the saturated soil  $v_{sat}$ ; (c) randomness in the local scour patterns that belong to the same local scour severity scenario (intra-scour severity scenario variability) as per Table 6; (d) randomness in the applied axial load  $N_{LL}$  (due to the variability of the traffic loads) and (e) randomness in the capacity thresholds as per Table 3. In particular, the soil shear modulus  $G_s$  [73], the Poisson's ratio  $v_{sat}$ , and the live load axial force  $N_{LL}$  were assumed to be uniformly distributed, in the absence of pertinent data to support a more elaborate probabilistic model. Their median and coefficient of viriation (CoV) estimates are summarised in Table 5 [77]. Uncertainties associated with the geometric properties of the investigated bridge pier and its foundation are assumed to be negligible and hence were disregarded.

Further to the above, randomness in the total scour was accounted for by considering four local scour scenarios (i.e., low, moderate, extensive and severe), each one of them associated with different scour patterns. The latter essentially implies that, for the baseline pier, fragility curves will be produced for four scour severity scenarios, where each scour severity scenario accounts for the randomness associated with the scour pattern. The different scour patterns considered herein (Table 2) account for a number of characteristic scour variations that

**Table 5**Statistical parameters of the uncertain properties.

Uncertain property	Notation	Distribution	Median	CoV
Soil shear modulus	$G_s$	Uniform	50	30 %
Poisson's ratio	$v_{sat}$	Uniform	0.35	20 %
Deck live load	$N_{LL}$	Uniform	746kN	30 %
Capacity thresholds	-	Lognormal	As per Table 3	35 %

could be observed within a certain severity scour scenario.

To account for the uncertainty associated with the definition of the capacity thresholds those were assumed to be lognormally distributed having a median value as per Table 5 and a CoV of 0.35 [56]. To generate the random bridge pier samples, the Latin Hypercube Sampling technique [78,79] was employed. A total of 100 bridge samples were produced to capture the randomness in demand due to axial load and uncertain soil properties (assuming zero correlation between the shear modulus and the Poisson's ratio) . Each bridge pier sample realisation was analysed for all the considered scour patterns that are presented in Table 2.

#### 6.3. Demand assessment

The response of the piers is evaluated through incremental static analysis, a method that is extensively used in earthquake engineering for assessing the deformation demands imposed to a structural system by the seismic motion [80]. Herein, we have transplanted this method from earthquake to flood engineering by introducing the so-called in this study incremental flood analysis (IFA). IFA was coined here to provide a descriptive means of the bridge pier flood performance under the lateral loads that are exerted by the hydrodynamic forces. The IFA was undertaken by subjecting the piers to an incrementally scaled (equivalent) hydrodynamic lateral force pattern (i.e., the inverse triangle shown in Fig. 2 and Fig. 5) up to collapse due to global (i.e., geometric) instability as a result of overturning. Pier samples generated using the statistical parameters shown in Table 5 are analysed for certain  $h_f$  and scour scenarios, each one depicting variations of local scour patterns of similar severity. The computed IFA curves are used to pair the monitored EDP with hydrodynamic loading. The underlying relationship between  $v_m$ and the applied hydrodynamic loading shown in Eq. (2) allows to express the IFA results in terms of  $v_m$ . At the same time,  $h_f$  is a variable to define the hydrodynamic force as per Eq. (2), thus forming the proposed vector flood IM. For a certain  $h_f$ , one may compute the flood velocities  $v_m$  and hence translate the vertical axis of the curve from hydrodynamic force to the vector IM  $\{v_m, h_f\}$ . Fig. 7 illustrates an IFA curve in the transverse direction of lateral loading, for the stiff pier under investigation (Fig. 6) and  $h_f/h_p = 1.0$ .

### 6.4. Numerical investigation

#### 6.4.1. Effect of local scour on the pier-foundation stiffness

The removal of soil around and under the foundation reduces the stiffness of the pier-foundation system. The stiffness reduction directly affects (i.e., reduces) the frequency of the system [42]. Natural period shifts of the bridge piers were used in past studies as post-earthquake damage predictors [81] as well as a proxy for detecting the development of scour in bridge foundations [82].

Fig. 8a illustrates the changes in the fundamental frequency (f) of the pier for the 18 considered local scour patterns (Cases 2-19) and the Case 1 that reflects the maximum global scour case (but without any local scour) for completeness, using the so-called "mean" bridge pier model, i. e., the model having all the uncertain properties set to their mean values.

<sup>\*\*</sup> (L > B).

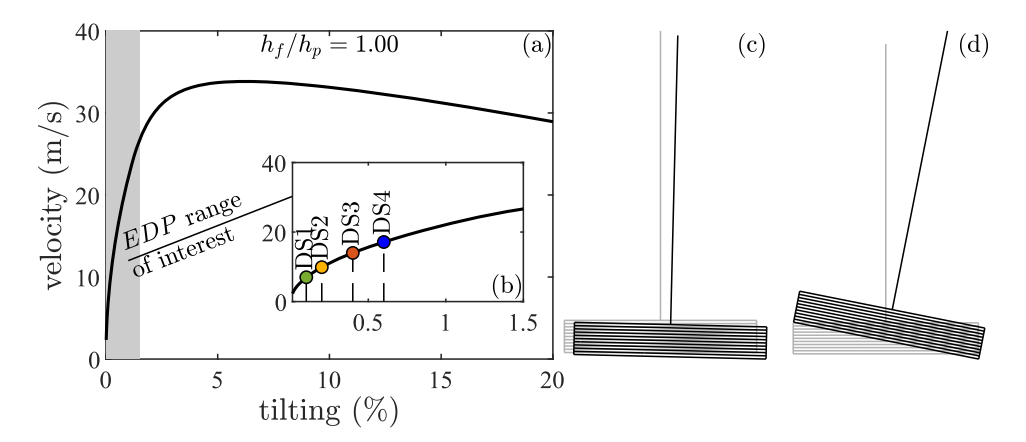


**Fig. 7.** (a) IFA curve for the case study pier and  $h_f/h_p=1.0$ ; (b) IFA curve zoom at the EPD range of interest, featuring the damage state capacity thresholds presented in Table 3; (c) deflected shape (exaggerated displacements) for the DS4 tilting capacity of 0.6 %; (d) deflected shape at global geometric instability. The results refer to a randomly chosen case with 80 % upstream scour, 40 % downstream scour and no under-scour (see also Fig. 2a).

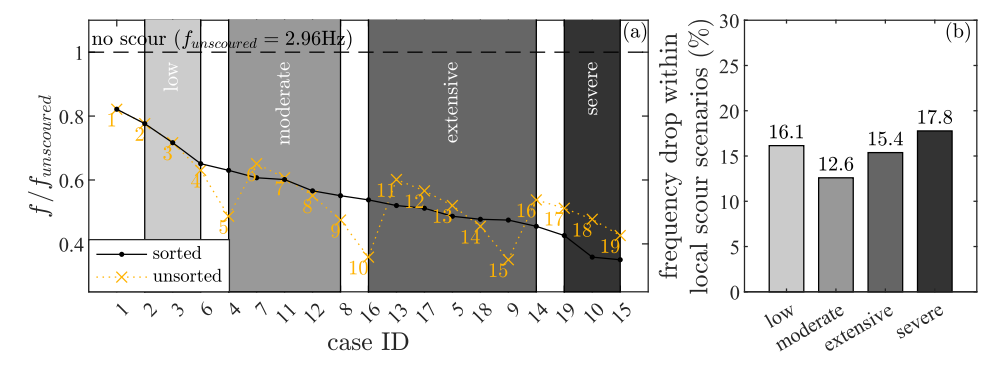


Fig. 8. Fundamental frequencies of the "mean" case study bridge pier analysed for different local scour patterns (case ID 2-19). The frequencies are normalised by the frequency of the unscoured case ("no scour", Case 0) and the local scour patterns are presented in descending order in terms of their fundamental frequency.

The results are normalised to the fundamental frequency of the completely unscoured case  $(f_{unscoured})$ , i.e. Case 0 as per Table 2. According to Fig. 8a, the fundamental frequency of the bridge pier drops as the local scour severity increases, because the stiffness of the bridge-foundation system decreases. This observation is in line with past studies, such as that of Tubaldi et al. [76] that investigated the effect of

scour on the frequencies of bridge piers with shallow foundations to consequently shed light on vibration-based techniques for bridge scour identification. Similar observations regarding the effect of scour on the overall stiffness of the system were also made by Guo [83]. The observations made with regard to the bridge pier frequency changes due to the different implemented local scour patterns will be exploited in the following section for pairing the local scour patterns with the local scour

**Table 6**Assignment of local scour patterns to local scour severity scenarios based on the allowable frequency drop within the same local scour bin (Fig. 8b); the scour patterns associated with the minimum and maximum frequencies that define the frequency drop in each local scour scenario appear in bold.

Case ID	Pattern ID	Upstream	Downstream	Under-scour (Upstream)	Scour severity	Frequency drop (%)
1	N/A	0 %	0 %	0 %	Max global scour (no local scour)	N/A
2	P1	20 %	20 %	0 %	Low	16.1
3	P2	40 %	40 %	0 %		
6	Р3	100 %	0 %	10 %		
4	P4	60 %	60 %	0 %	Moderate	12.6
7	P5	100 %	20 %	10 %		
8	P6	100 %	40 %	10 %		
11	P7	100 %	0 %	20 %		
12	P8	100 %	20 %	20 %		
5	P9	80 %	80 %	0 %	Extensive	15.4
9	P10	100 %	60 %	10 %		
13	P11	100 %	40 %	20 %		
14	P12	100 %	60 %	20 %		
16	P13	100 %	0 %	<b>30</b> %		
17	P14	100 %	20 %	30 %		
18	P15	100 %	40 %	30 %		
10	P16	100 %	80 %	10 %	Severe	17.8
15	P17	100 %	80 %	20 %		
19	P18	100 %	60 %	30 %		

severity scenarios.

#### 6.4.2. Definition of local scour scenarios

The response of the benchmark bridge pier was evaluated for four local scour scenarios of increasing severity, i.e., minor, moderate, extensive and severe. Each scenario, presented in Table 6, accounts for several local scour patterns (Table 2 and Table 6). To assign each local scour pattern to a specific local scour scenario, bridge pier frequencies associated with a specific local scour pattern were rearranged in descending order, as illustrated in Fig. 8a. Subsequently, four local scour bins (i.e., minor, moderate, extensive and severe) were created, containing local scour patterns that have relatively similar frequencies. The allowable differences in the frequency drop (i.e., percentage (%) difference between the maximum and minimum frequency within the same bin) within a single local scour bin in this study were set in the order of ~15 %, based on engineering judgement, as shown in Fig. 8b. To this end, the first three frequencies (highest frequencies among the investigated bridge pier models) were paired with the low scour severity scenario. The next five frequencies were paired to the moderate scour severity scenario and similarly the remaining seven and three cases were assigned to the extensive and severe scour scenarios, respectively.

The evaluation of the bridge flood vulnerability at different scour severity scenarios, essentially allows for the assessment of: (a) the current state of an existing bridge, should scour be already present around the pier foundation; and (b) the future state of an existing (with or without scour) or a new (without scour) bridge on account that no scour mitigation measures (e.g., bed armouring methods) are taken to prevent the further development or the initiation and development of scour during successive flood incidents over the years. In the latter case,

reasonable estimates for the scour depth and progression over time may be made utilising scour models that are already available in the literature (e.g., [84,85]).

It should be underlined that the defined local scour patterns are by no means exhaustive, and one might extent the considered cases to more accurately capture the intra-scour severity scenarios variability, as per the needs of the undertaken fragility assessment. Moreover, the underscour in the considered patterns was limited to 30 %. This essentially means that the considered scour patterns do not capture the failure mode related to the bridge overturning against the upstream side. This failure mode is triggered solely by the scour severity, in cases which the destabilising effect of gravity forces exceeds the effect of the hydraulic actions, that now act as restoring forces.

#### 6.5. Analysis matrix

An analysis matrix is formed to capture the effect of the uncertainties discussed in previous sections of this paper on the response of bridges against flooding. Using the parameters reported in Table 5 as well as the Latin Hypercube Sampling technique [79], 100 bridge pier samples are generated. Each bridge pier sample is analysed for three water depth ratios of  $h_f/h_p = \{0.50,\ 0.75,\ 1.00\}$  and the scour patterns shown in Table 2. In total,  $100\times3\times20=6000$  IFAs were performed. The IFA curve depicts how the monitored EDP varies with increasing levels of the hydrodynamic loading that is exerted to the pier due to a flood incident. For a certain flood height, the hydrodynamic load is paired to the mean flood velocity  $\nu_m$ , as discussed in Section 5.3 (Fig. 7).

Considering the pier titling as the monitored EDP, Fig. 9 illustrates the IFA curves of the bridge pier samples, evaluated for four considered

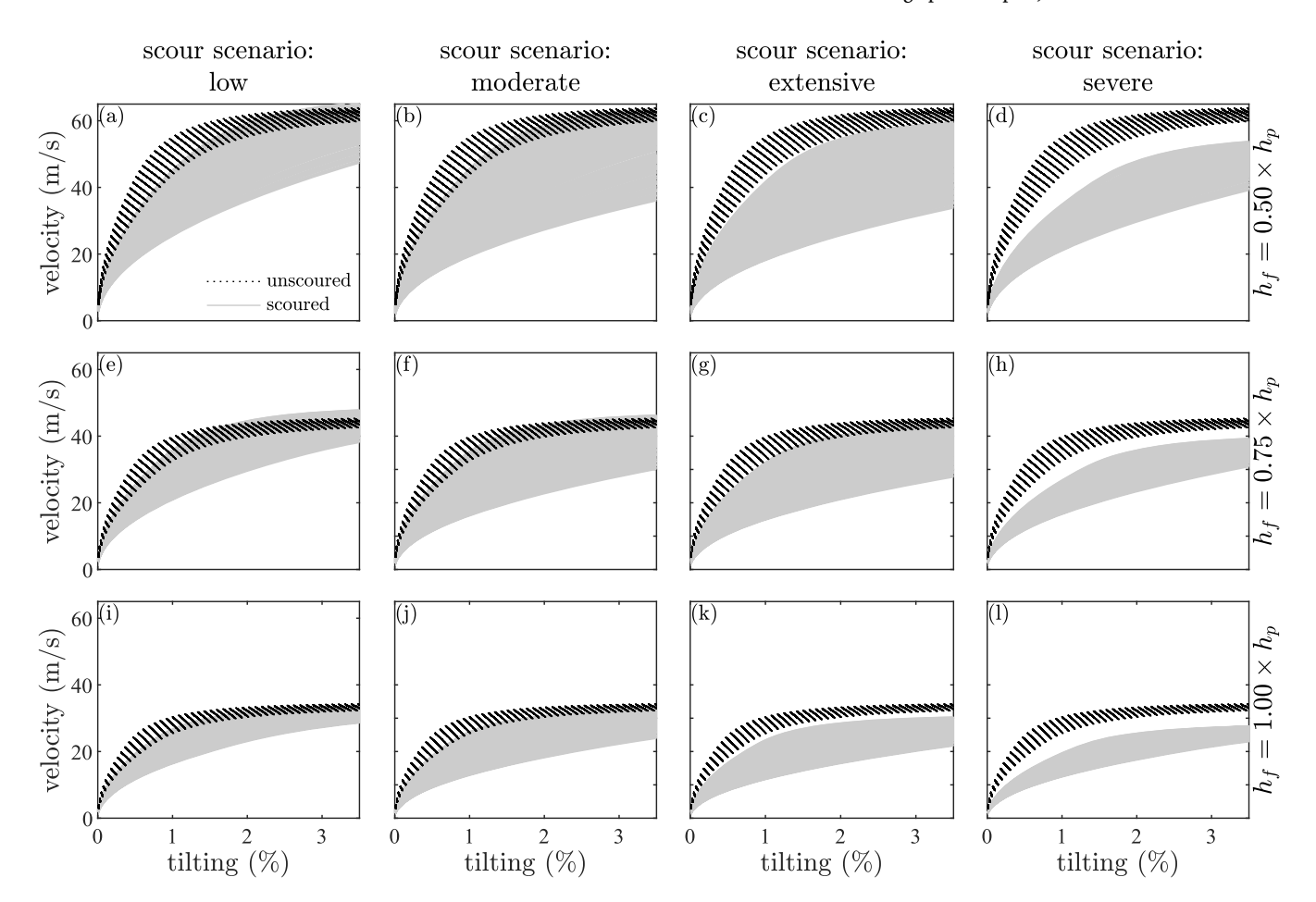


**Fig. 9.** IFA curves of the benchmark bridge pier samples per scour severity scenario: (a-d)  $h_f/h_p = 0.50$ ; (e-h)  $h_f/h_p = 0.75$ ; (i-l)  $h_f/h_p = 1.00$ ; the black dotted lines correspond to the "intact" (i.e., unscoured) bridge pier samples.

scour scenarios (Table 6) and three distinct inundation depths. As can be inferred by the plots, the effect of randomness on the soil properties and the traffic loads as well as the impact of the local scour pattern variability, becomes more significant for the moderate and the extensive local scour scenarios, whereas the response is less variable for the two extreme local scour scenario cases, i.e., low and severe. It should be noted that the  $\nu_m$  in the IFA curves reach high values which might be unrealistic, however they are presented here for illustration purposes. Still, higher  $\nu_m$  than those reported in the literature could be developed if large debris accumulation restricts the water flow, essentially leading to a local increase of the flood velocity at the vicinity of the pier [86,87].

#### 6.6. Response statistics

Fig. 10 illustrates the response statistics evaluated over a range of flood intensities, considering the titling of the bridge pier as an EDP. The spectrum of responses covers cases that range from the initiation of titling up to higher drifts of the pier (Fig. 7). Fig. 10(a-d) depict the median EDP responses at the four investigated scour severity scenarios (Table 6), while Fig. 10(e-h) the pertinent dispersion of the IM conditioned on the EDP response,  $\beta_{EDP|IM}$  (evaluated as the standard deviation of the data natural logarithms). The different curves in each scour severity scenario correspond to three distinct flood heights, the latter being expressed as a ratio of the pier height, i.e.,  $h_f/h_p = \{0.50,\ 0.75,\ 1.00\}$ .

As can be inferred by inspecting Fig. 10, the most severe scour scenarios are associated with higher median EDP|IM demands. This is reasonable, since most severe scour scenarios are associated with a higher vulnerability, in the sense of propensity to damage of the bridge pier to flood exerted forces. In other words, for a given  $h_f$ , comparing a severely scoured shallow foundation pier with a less scoured one, lower flow velocities are required for the former to develop the same EDP with the latter. Further to the above, with reference to the same local scour severity scenario, lower flood heights result in lower EDP demands for the same flood velocity level. Last, the sudden increase in dispersion observed in Fig. 10(e-h) refers to initiation of the foundation uplift, beyond which the response naturally becomes more variable.

#### 6.7. Flood fragility curves

The outcomes of the fragility study are presented in Fig. 11 for all

four considered Damage States that are paired with 0.1 % (DS1), 0.2 % (DS2), 0.4 % (DS3) and 0.6 % (DS4) capacity thresholds for the pier tilting. The median as well as the total dispersion of the fragilities  $\beta_{tot}$  evaluated as per Eq. (5) shown in Fig. 11, are summarised in Table 7 for all considered scour scenarios, three representative flood heights and the damage states of Table 3. It should be noted that the utilisation of a vector IM results in fragility surfaces (e.g., [88]). However, for better clarity slices from these surfaces were taken at three characteristic inundation depth heights (i.e.,  $\nu_m | h_f$  slices) and hence the results are offered in the form of two-dimensional fragility curves. Fig. 12 is also provided in support of the results reported in Table 7, to visualise the effect of the chosen parameters.

As expected, less severe local scour scenarios can sustain higher flood velocities, a condition that essentially relates to a less vulnerable structural system. In fact, moving from severe to low local scour scenarios, the flood fragility of the pier drops. The latter is more evident for inundation depths that do not reach the top of the bridge pier, in which cases especially the low-scour scenario is associated with high flood velocities almost across all DSs. For instance, the flood velocity associated with a 50 % probability of exceeding the DS1 for the low scour scenario is approximately equal to 11 m/s when  $h_f/h_p = 0.5$  and 9 m/s when  $h_f/h_p = 0.75$  (see Table 7). The propensity of the pier to any floodinduced damage is further reduced for the unscoured case. In the case of an unscoured pier that is affected by a  $h_f/h_p = 1.0$  flood, the water velocity for 1 % probability of exceedance in DS3 and DS4 is 16.2 m/s and 19.9 m/s, respectively. Hence, for shallow foundation bridge piers, a mitigation measure that one needs to prioritise, is to protect the foundations from being scoured and fill any scour holes from past events. As an additional example, assuming that the case study bridge crosses a river in which the 500-year flood has a mean flood velocity equal to 8 m/ s and an inundation depth of 9 m (i.e.,  $h_f/h_p = 1.0$ ), according to the fragilities of Fig. 11 for the severe scour severity scenario, the probabilities that the bridge is in individual damage states DS1, DS2, DS3 and DS4 are 21.1 %, 72.7 %, 5.8 % and 0.2 %, respectively. For the aforementioned example, increasing the flood velocity from 8 m/s to 9 m/s yields an increased probability of being in DS3 of 20.5 % whereas for 10 m/s the same quantity increases to 39.8 %. Interpretation of the above observations, from a practical standpoint, may be accomplished via considering that during a severe flood incident, the water velocity usually ranges from 3 to 10 m/s [30]. The velocity values reported

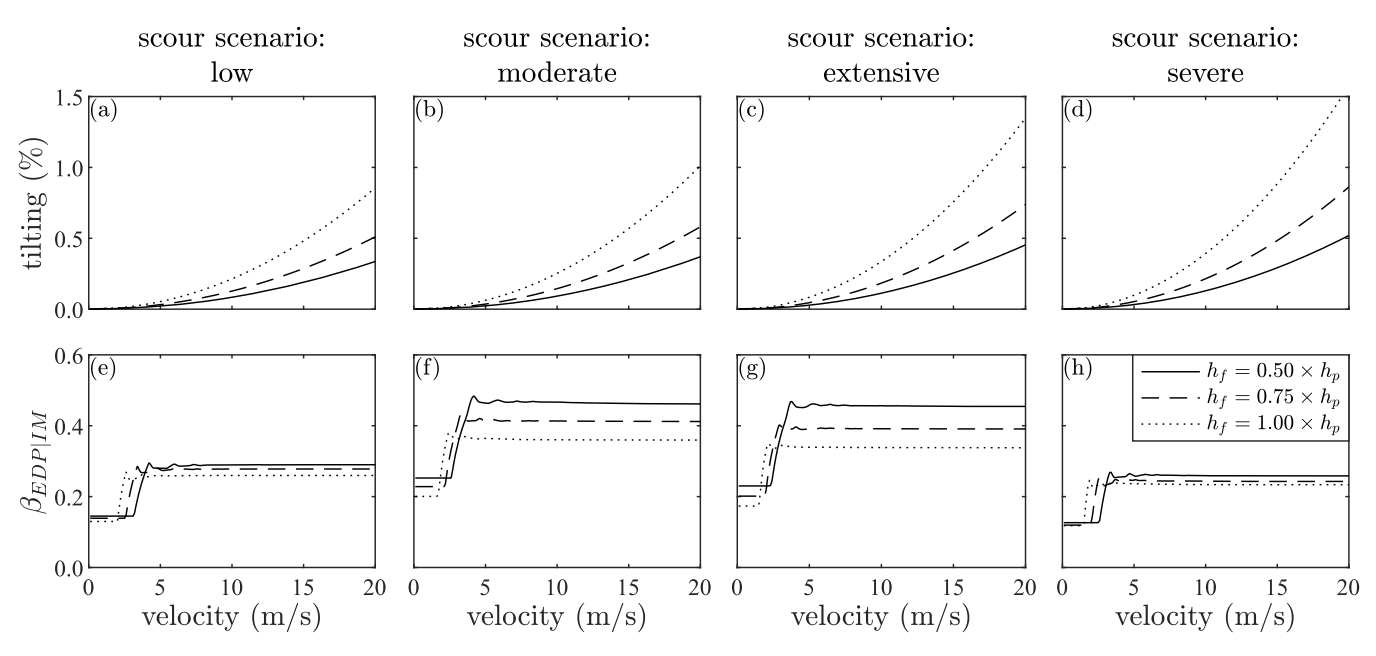


Fig. 10. Median EDP response (a-d) and dispersion (e-h) estimates over a range of flood IM levels for three distinct  $h_f/h_p$  and four local scour scenarios (Table 6).

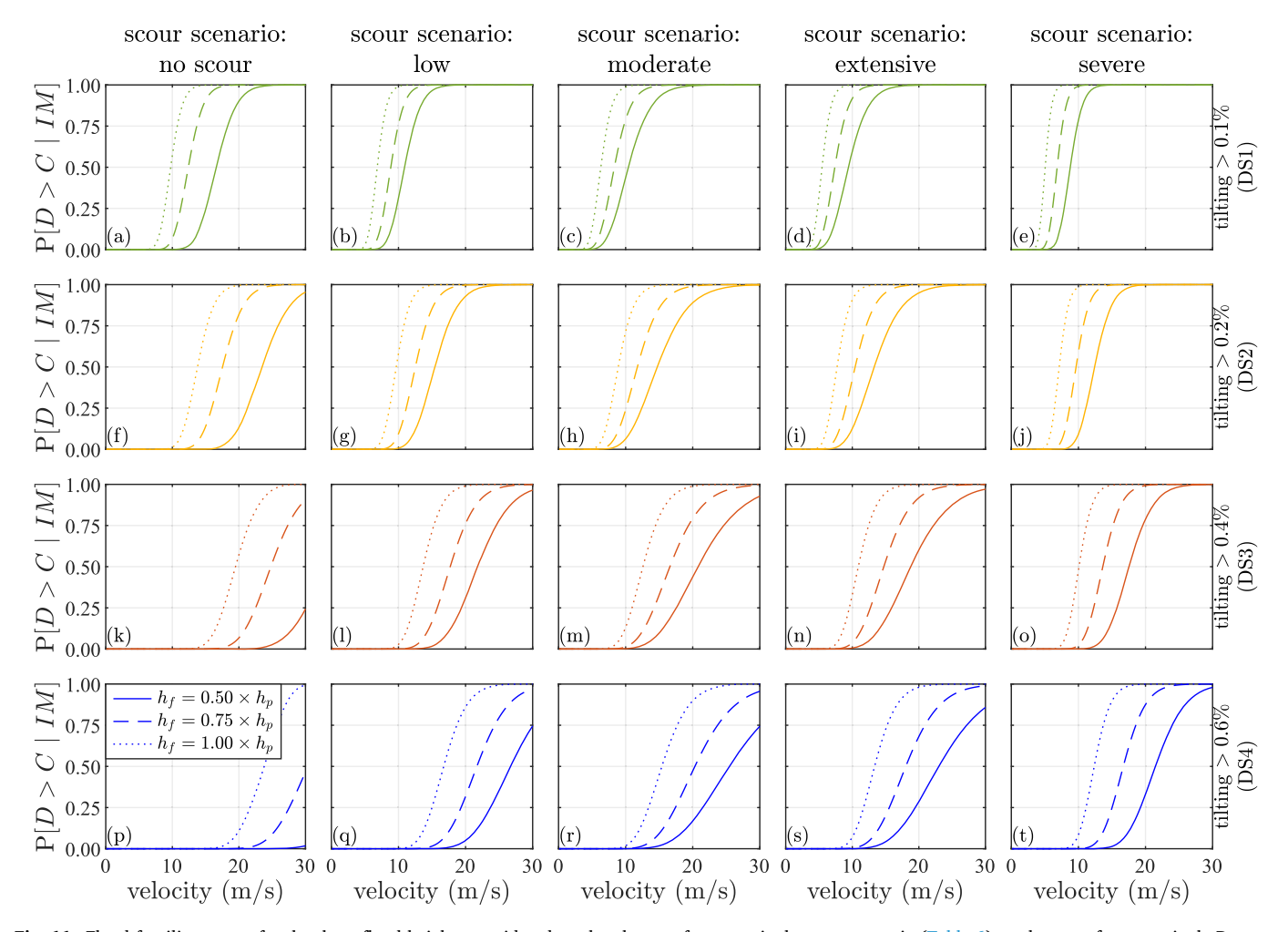


Fig. 11. Flood fragility curves for the three flood heights considered: each column refers to a single scour scenario (Table 6); each row refers to a single Damage State (Table 3).

**Table 7**Median and total dispersion flood fragility parameters.

Scour severity	$h_f/h_p$	DS1		DS2		DS3		DS4	
		$\widehat{\nu_m}$	$\beta_{tot}$	$\widehat{\nu_m}$	$\beta_{tot}$	$\widehat{\nu_m}$	$\beta_{tot}$	$\widehat{\nu_m}$	$\beta_{tot}$
No scour	0.50	16.6	0.14	23.5	0.14	33.2	0.14	40.6	0.14
	0.75	12.4	0.14	17.5	0.14	24.8	0.14	30.4	0.13
	1.00	9.7	0.14	13.8	0.14	19.5	0.14	23.8	0.13
Low	0.50	10.9	0.18	15.4	0.18	21.8	0.18	26.7	0.18
	0.75	8.9	0.17	12.5	0.17	17.7	0.17	21.7	0.17
	1.00	6.8	0.16	9.7	0.16	13.7	0.16	16.7	0.16
Moderate	0.50	10.4	0.25	14.7	0.25	20.8	0.25	25.5	0.25
	0.75	8.3	0.23	11.8	0.23	16.6	0.23	20.3	0.23
	1.00	6.3	0.20	8.9	0.20	12.6	0.20	15.4	0.20
Extensive	0.50	9.4	0.25	13.3	0.25	18.8	0.25	23.0	0.25
	0.75	7.4	0.22	10.4	0.22	14.7	0.22	18.0	0.22
	1.00	5.4	0.22	7.7	0.20	10.9	0.20	13.4	0.20
Severe	0.50	8.8	0.16	12.4	0.16	17.5	0.16	21.5	0.16
	0.75	6.8	0.16	9.6	0.16	13.6	0.16	16.7	0.16
	1.00	5.0	0.16	7.1	0.15	10.1	0.15	12.4	0.15

herein are slightly higher; yet, it should be kept in mind that debris accumulation was disregarded, a condition that if it had been accounted for, would have been expected to reduce the median velocity capacities. Furthermore, the evaluated fragilities are specific to the assumptions made with regard to the soil conditions.

As a final remark, it should be pointed out in a flood fragility assessment depicting a representative fragility that reflects to the most representative or likely scour severity scenario for the case at hand,

requires from the engineers to consider the scour susceptibility at the bridge location of interest making appropriate allowances for climate change [89]. If in doubt conservative assumptions should be made, unless scour countermeasures are or will be implemented.

# 7. Conclusions

We provided a new methodology for evaluating analytical flood

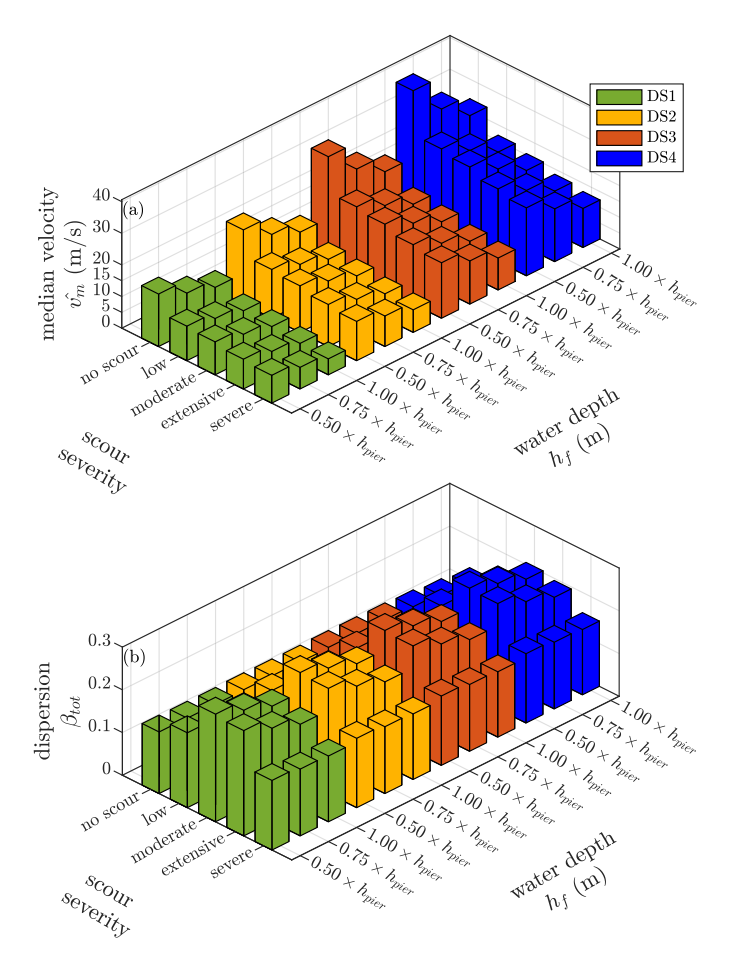


Fig. 12. Flood fragility statistics per scour scenario and flood height for the benchmark bridge pier: (a) median velocity; (b) total dispersion.

fragility curves of bridge piers with an integrated approach that accounted for critical variable parameters. This research is in response to the urgent need for developing generalised fragility models for bridges exposed to floods-the most critical cause of bridge failure worldwide. Although bridge fragility assessment is relatively mature for other natural hazards, when it comes to floods there are only few studies available in the international literature that provide detailed guidelines. This is a knowledge gap, because fragilities constitute an important element in modern quantitative risk assessment methodologies [90]. The investigation was conducted for shallow foundations of bridges piers, while the method can be tailored to other bridge pier typologies, e. g., piled and caisson foundations, and for variable bridge failure modes with appropriate adjustments. For characterising the intensity of the flood hazard, a new vector intensity measure was proposed that accounts for both the water velocity and the inundation depth, normalised to the pier height. To account for the variability and increase of bridge flood vulnerability due to the accumulation of scour to past flood events, the fragilities were evaluated for several scour scenarios of increasing severity that were defined accounting for the intra-scenario scour variability. The latter represents different scour patterns which may reflect the same scour severity scenario. To associate scour patterns with certain scour severity scenarios, the natural frequencies of the piers were taken into account, as an indicator of the pier-foundation stiffness loss due to the presence of scour.

It was demonstrated that flood fragility increases with increasing inundation depth and scour severity. The flood fragility assessment framework presented herein is suitable for bridge-specific assessments, and for studies that require the analysis of a large portfolio of bridges. It could also assist the process of delivering new bridge designs with

homogeneous probabilities of being in or exceeding certain damage states when exposed to the flood hazard (see Monti et al. [91]). Owing to the simplified modelling approach, the methodology presented herein has the potential to provide flood fragility information for a wide range of bridge geometries. Through suitable modifications of the model adopted, additional failure modes can be considered, towards a holistic flood risk assessment framework for bridges, where a spectrum of representative bridge classes are covered.

The unified flood fragility framework that was presented in this research study employs two-dimensional (2D) reduced-order bridge pier models. This modelling approach leads also to simplifications with regards to definition of the scour patterns geometries that are likely to develop around the foundation of the pier, that would have been more accurately depicted if a three-dimensional (3D) model was adopted. In particular, the scour development is only accounted for in the direction parallel to the flow (both upstream and downstream) and was disregarded in the orthogonal direction. This was a conscious choice on account of: (a) 2D reduced-order models are often adopted in fragility studies that involve numerous structural analyses since it is acceptable to trade some accuracy for efficiency, and (b) the scour development parallel to the direction of the flow, in cases that the pier is aligned with the flow (or not severely skewed), like the case that was investigated here, is the one that mostly determines its flood performance. However, should knowledge in the pertinent domain is advanced and sufficient resources are available, the proposed framework could accommodate all levels of modelling accuracy.

The methodology was also presented by assuming elastic bridge behaviour, yet accounting for geometric nonlinearities, and linear behaviour for the soil. For larger tilting levels, which were not of interest to this study, or in cases that the bridge pier is likely to develop inelasticity during the tilting levels of interest, these assumptions do not hold. Yet, for the investigated bridge typology, the considered damage states and the assumed capacity thresholds are representative based on damage states of real bridge piers. The framework was presented for a single bridge failure mechanism. To assess the reliability of the entire bridge, all plausible failure mechanisms, e.g., deck unseating, damages in the abutments, can be considered depending on the level of the sought accuracy. Nevertheless, deck unseating requires the latter to be at least partially submerged during the flood, a condition that was not accounted for herein, since the maximum inundation depth considered was limited to the pier height. In case of inundation depths that could result in deck unseating and relatively lightweight decks, the flood velocities leading to bridge failure can be significantly reduced [86]. In any case, detailed modelling should be applied for bridges that are identified by means of the proposed method as being the most vulnerable within the investigated network.

The proposed unified framework is suitable for both bridge-specific and class flood fragility assessment studies. This is mainly because it employs reduced-order bridge component numerical models as well as an informative non-structure, non-location specific IM to characterise the severity of the hydraulic forces. Owing to the simplicity of the numerical model, several bridge component variations (i.e., index bridge components) that could capture the flood performance of a bridge class of interest (i.e., the intra-class variability) may be analysed by means of the newly introduced IFA method, to reveal their flood induced response at incrementally increased intensity levels and consequently evaluate their flood fragility. Uncertainties associated with the foundation scour are also addressed in the proposed framework in a novel manner, by means of evaluating the statistics of the bridge pier response of interest (and hence the flood fragilities) considering different representative foundation scour scenarios of increased severity. The latter allows a direct appreciation of the flood performance downgrade due to the presence of scour and hence the benefits stemming from the implementation of scour protection measures. The proposed methodology also accounts for the intra-scour severity scenario variability though considering several scour patterns that reflect the same scour severity level. Those scour patterns are paired to specific scour severity scenarios by considering their impact on the pier-foundation system stiffness. Finally, the proposed methodology is suitable for developing response datasets through analysing several bridge component variations in a fraction of time that would have required for more refined bridge pier numerical representations. Those datasets can be then exploited either for developing closed-form response prediction equations or for enabling response predictions via training a machine learning algorithm.

#### CRediT authorship contribution statement

Athanasia K. Kazantzi: Writing – review & editing, Writing – original draft, Visualization, Validation, Supervision, Software, Methodology, Investigation, Conceptualization. Konstantinos Bakalis: Writing – review & editing, Visualization, Validation, Software, Methodology, Investigation, Formal analysis, Conceptualization. Stergios-Aristoteles Mitoulis: Writing – review & editing, Supervision, Funding acquisition, Conceptualization.

#### Declaration of competing interest

The authors declare that they have no known competing financial interests or personal relationships that could have appeared to influence the work reported in this paper.

#### Acknowledgements

This study received funding by the UK Research and Innovation (UKRI) under the UK government's Horizon Europe funding guarantee [grant agreement No: 10062091]. This is the funding guarantee for the European Union HORIZON-MISS-2021-CLIMA-02 [grant agreement No: 101093939] RISKADAPT - Asset-level modelling of risks in the face of climate-induced extreme events and adaptation.

The authors would also like to acknowledge funding by the UK Research and Innovation (UKRI) under the UK government's Horizon Europe funding guarantee [grant agreement No: 101086413, EP/Y003586/1, EP/Y00986X/1, EP/X037665/1]. This is the funding guarantee for the European Union HORIZON-MSCA-2021-SE-01 [grant agreement No: 101086413] ReCharged - Climate-aware Resilience for Sustainable Critical and interdependent Infrastructure Systems enhanced by emerging Digital Technologies.

The publication of the article in OA mode was financially supported by HEAL-Link.

#### Data availability

Data will be made available on request.

#### References

- Zhang G, Liu Y, Liu J, Lan S, Yang J. Causes and statistical characteristics of bridge failures: a review. J Traffic Transp Eng 2022;9:388–406. https://doi.org/10.1016/ i itte 2021 12 003
- [2] Hunt B. Monitoring scour critical bridges. Washington, D.C.: Transportation Research Board; 2009. https://doi.org/10.17226/22979.
- [3] Pregnolato M. Bridge safety is not for granted a novel approach to bridge management. Eng Struct 2019;196:109193. https://doi.org/10.1016/j. engstruct.2019.05.035.
- [4] Bezak N, Panagos P, Liakos L, Mikoš M. Brief communication: a first hydrological investigation of extreme August 2023 floods in Slovenia, Europe. Nat Hazards Earth Syst Sci 2023;23:3885–93. https://doi.org/10.5194/nhess-23-3885-2023.
- [5] He K, Yang Q, Shen X, Dimitriou E, Mentzafou A, Papadaki C, et al. Brief communication: Storm Daniel Flood impact in Greece 2023: mapping crop and livestock exposure from SAR. Nat Hazards Earth Syst Sci Discuss 2023. https://doi. org/10.5194/nhess-2023-173
- [6] Dimitriou E, Efstratiadis A, Zotou I, Papadopoulos A, Iliopoulou T, Sakki G, et al. Post-analysis of Daniel extreme flood event in Thessaly, Central Greece: practical lessons and the value of state-of-the-art water-monitoring networks. Water 2024; 16:980. https://doi.org/10.3390/w16070980.

- [7] Ekathimerini. Storm Daniel repairs to cost 6600 mln 2023. https://www.ekathimerini.com/news/1221089/storm-daniel-repairs-to-cost-e600-mln/(accessed April 8, 2024).
- [8] Loli M, Kefalas G, Dafis S, Mitoulis SA, Schmidt F. Bridge-specific flood risk assessment of transport networks using GIS and remotely sensed data. Sci Total Environ 2022;850:157976. https://doi.org/10.1016/j.scitotenv.2022.157976.
- [9] Loli M, Mitoulis SA, Tsatsis A, Manousakis J, Kourkoulis R, Zekkos D. Flood characterization based on forensic analysis of bridge collapse using UAV reconnaissance and CFD simulations. Sci Total Environ 2022;822:153661. https:// doi.org/10.1016/j.scitotenv.2022.153661.
- [10] Singh P, Amekudzi-Kennedy A, Ashuri B, Chester M, Labi S, Wall TA. Developing adaptive resilience in infrastructure systems: an approach to quantify long-term benefits. Sustain Resilient Infrastruct 2023;8:26–47. https://doi.org/10.1080/ 23789689.2022.2126631.
- [11] Pervaiz F, Hummel MA. Effects of climate change and urbanization on bridge flood vulnerability: a regional assessment for Harris County, Texas. Nat Hazards Rev 2023;24:1–10. https://doi.org/10.1061/nhrefo.nheng-1720.
- [12] Boakye J, Guidotti R, Gardoni P, Murphy C. The role of transportation infrastructure on the impact of natural hazards on communities. Reliab Eng Syst Saf 2022;219:108184. https://doi.org/10.1016/j.ress.2021.108184.
- [13] Sharma N, Gardoni P. Mathematical modeling of interdependent infrastructure: an object-oriented approach for generalized network-system analysis. Reliab Eng Syst Saf 2022;217:108042. https://doi.org/10.1016/j.ress.2021.108042.
- [14] Nocera F, Contento A, Gardoni P. Risk analysis of supply chains: the role of supporting structures and infrastructure. Reliab Eng Syst Saf 2024;241:109623. https://doi.org/10.1016/j.ress.2023.109623.
- [15] Koursari E, Wallace S. Infrastructure scour management: a case study for A68 Galadean Bridge, UK. In: Proceedings of the Institution of Civil Engineers - Bridge Engineering, 173; 2020. p. 42–9. https://doi.org/10.1680/jbren.18.00062.
- [16] Nemry F, Demirel H. Impacts of climate change on transport: a focus on road and rail transport infrastructures. EUR 25553 EN. Luxembourg: Publications Office of the European Union; 2012. https://doi.org/10.2791/15504. JRC72217.
- [17] Miyamoto International Inc. Increasing infrastructure resilience background report. https://documents1.worldbank.org/curated/en/620731560526509220/ pdf/Technical-Annex.pdf.
- [18] Muntasir Billah AHM, Shahria Alam M. Seismic fragility assessment of highway bridges: a state-of-the-art review. Struct Infrastruct Eng 2015;11:804–32. https://doi.org/10.1080/15732479.2014.912243.
- [19] Chen X, Ikago K, Guan Z, Li J, Wang X. Lead-rubber-bearing with negative stiffness springs (LRB-NS) for base-isolation seismic design of resilient Bridges: A Theoretical feasibility study. Eng Struct 2022;266:114601. https://doi.org/ 10.1016/j.engstruct.2022.114601.
- [20] Decò A, Frangopol DM. Risk assessment of highway bridges under multiple hazards. J Risk Res 2011;14:1057–89. https://doi.org/10.1080/ 13669877.2011.571789.
- [21] Argyroudis SA, Mitoulis SA. Vulnerability of bridges to individual and multiple hazards- floods and earthquakes. Reliab Eng Syst Saf 2021;210:107564. https://doi.org/10.1016/j.ress.2021.107564.
- [22] Foti S, Aimar M, Ciancimino A, Giordano L. Influence of scour of foundations on the seismic performance of bridges. In: SECED 2023 conference: earthquake engineering & dynamics for a sustainable future; 2023. https://www.seced.org.uk/index.php/seced-2023-proceedings/80-keynote-lectures/927-influence-of-s cour-of-foundations-on-the-seismic-performance-of-bridges.
- [23] Annad M, Zourgui NH, Lefkir A, Kibboua A, Annad O. Scour-dependent seismic fragility curves considering soil-structure interaction and fuzzy damage clustering: a case study of an Algerian RC Bridge with shallow foundations. Ocean Eng 2023; 275:114157. https://doi.org/10.1016/j.oceaneng.2023.114157.
- [24] Stefanidou S, Markogiannaki O, Mikes I, Fragiadakis M. Fragility analysis framework for bridges subjected to successive natural hazards. Struct Eng Int 2024; 34:45–54. https://doi.org/10.1080/10168664.2023.2273464.
- [25] Filizadeh R, Hernandez EM, Rosowsky DV. Risk-based framework for post-earthquake monitoring and evaluation of reinforced concrete bridges subject to multiple hazards. Reliab Eng Syst Saf 2024;245:109992. https://doi.org/10.1016/iress.2024.109992
- [26] Khandel O, Soliman M. Integrated framework for assessment of time-variant flood fragility of bridges using deep learning neural networks. J Infrastruct Syst 2021;27. https://doi.org/10.1061/(ASCE)IS.1943-555X.0000587.
- [27] Anisha A, Jacob A, Davis R, Mangalathu S. Fragility functions for highway RC bridge under various flood scenarios. Eng Struct 2022;260:114244. https://doi. org/10.1016/j.engstruct.2022.114244.
- [28] Anisha A, Sahu DK, Sarkar P, Mangalathu S, Davis R. High dimensional model representation for flood fragility analysis of highway bridge. Eng Struct 2023;281: 115817. https://doi.org/10.1016/j.engstruct.2023.115817.
- [29] Lee J, Lee Y-J, Kim H, Sim S-H, Kim J-M. A new methodology development for flood fragility curve derivation considering structural deterioration for bridges. Smart Struct Syst 2016;17:149–65. https://doi.org/10.12989/sss.2016.17.1.149.
- [30] Kim H, Sim S-H, Lee J, Lee Y-J, Kim J-M. Flood fragility analysis for bridges with multiple failure modes. Adv Mech Eng 2017;9:168781401769641. https://doi.org/ 10.1177/1687814017696415.
- [31] Ahamed T, Duan JG, Jo H. Flood-fragility analysis of instream bridges consideration of flow hydraulics, geotechnical uncertainties, and variable scour depth. Struct Infrastruct Eng 2021;17:1494–507. https://doi.org/10.1080/ 15732479.2020.1815226.
- [32] Rincon R, Padgett JE. Fragility modeling practices and their implications on risk and resilience analysis: from the structure to the network scale. Earthq Spectra 2024;40:647–73. https://doi.org/10.1177/87552930231219220.

- [33] Porter K, Cho I. Characterizing a building class via key features and index buildings for class-level vulnerability functions. In: 11th International Conference on Structural Safety & Reliability (ICOSSAR). New York, NY: Columbia University; 2013
- [34] Kazantzi AK, Vamvatsikos D. Intensity measure selection for vulnerability studies of building classes. Earthq Eng Struct Dyn 2015;44:2677–94. https://doi.org/ 10.1002/ege.2603.
- [35] Stefanidou SP, Kappos AJ. Bridge-specific fragility analysis: when is it really necessary? Bull Earthq Eng 2019;17:2245–80. https://doi.org/10.1007/s10518-018-00525-9.
- [36] Biazar S, Kameshwar S, Balomenos GP. Multi-hazard fragility modeling framework for bridges with shallow foundations subjected to earthquake, scour, and vehicular loading. Soil Dyn Earthq Eng 2024;178:108482. https://doi.org/10.1016/j. soildyn.2024.108482.
- [37] D'Ayala D, Meslem A, Vamvatsikos D, Porter K, Rossetto T. Guidelines for analytical vulnerability assessment - low/mid-rise buildings. Vulnerability Global Component Project: 2015. https://doi.org/10.13117/GEM.VULN-MOD.TR2014.
- [38] Nofal OM, van de Lindt JW, Do TQ. Multi-variate and single-variable flood fragility and loss approaches for buildings. Reliab Eng Syst Saf 2020;202:106971. https://doi.org/10.1016/j.ress.2020.106971.
- [39] FEMA. Hazus flood technical manual (5.1). 2022. https://www.fema.gov/sites/default/files/documents/fema\_hazus-flood-model-technical-manual-5-1.pdf. Washington, D.C.
- [40] Arora RK, Banerjee S. Reliability-based approach for fragility assessment of bridges under floods. Struct Eng Mech 2023;88:311–22. https://doi.org/10.12989/ sem.2023.88.4.311.
- [41] Nofal OM, van de Lindt JW. High-resolution flood risk approach to quantify the impact of policy change on flood losses at community-level. Int J Disaster Risk Reduct 2021;62:102429. https://doi.org/10.1016/j.ijdrr.2021.102429.
- [42] Antonopoulos C, Tubaldi E, Carbonari S, Gara F, Dezi F. Dynamic behavior of soil-foundation-structure systems subjected to scour. Soil Dyn Earthq Eng 2022;152: 106969. https://doi.org/10.1016/j.soildyn.2021.106969.
- [43] Mao Q, Mazzotti M, Furkan M, Hicks A, Bartoli I, Aktan E. Characterization of bridge substructures explored by leveraging structural identification of a scaled bridge model. Eng Struct 2021;246:112953. https://doi.org/10.1016/j. engstruct.2021.112953.
- [44] Watanabe K, Nakagawa F, Sanagawa T, Chevalier C. Hydraulic model test on destabilization process of river bridge pier caused by local scour. In: 11th International Conference on Scour and Erosion; 2023. https://www.issmge.org/pu blications/publication/hydraulic-model-test-on-destabilization-process-of-river-br idge-pier-caused-by-local-scours.
- [45] McKenna F. Object oriented finite element programming frameworks for analysis, algorithms and parallel computing. CA: Univ. of California at Berkeley; 1997. https://opensees.berkeley.edu/OpenSees/doc/fmkdiss.pdf.
- [46] McKenna F. OpenSees: a framework for earthquake engineering simulation. Comput Sci Eng 2011;13:58–66. https://doi.org/10.1109/MCSE.2011.66.
- [47] Tubaldi E, Macorini L, Izzuddin BA. Three-dimensional mesoscale modelling of multi-span masonry arch bridges subjected to scour. Eng Struct 2018;165:486–500. https://doi.org/10.1016/j.engstruct.2018.03.031.
- [48] Gazetas G. Formulas and charts for impedances of surface and embedded foundations. J Geotech Eng 1991;117:1363–81. https://doi.org/10.1061/(ASCE) 0733-9410(1991)117:9(1363).
- [49] FEMA. Prestandard and commentary for the seismic rehabilitation of buildings. In: FEMA-356, prepared by the building seismic safety council for the federal emergency management agency, Washington, D.C.; 2000. https://www.nehrp. gov/pdf/fema356.pdf.
- [50] Sextos A, Faraonis P, Zabel V, Wuttke F, Arndt T, Panetsos P. Soil-bridge system stiffness identification through field and laboratory measurements. J Bridge Eng 2016;21. https://doi.org/10.1061/(ASCE)BE.1943-5592.0000917.
- [51] Faraonis P, Sextos A, Chatzi E, Zabel V. Model updating of a bridge-foundation-soil system based on ambient vibration data. In: Proceedings of the 1st international conference on uncertainty quantification in computational sciences and engineering (UNCECOMP 2015). Athens: Institute of Structural Analysis and Antiseismic Research School of Civil Engineering National Technical University of Athens (NTUA) Greece; 2015. p. 177–88. https://doi.org/10.7712/ 120215.4262.709.
- [52] Klinga JV, Alipour A. Assessment of structural integrity of bridges under extreme scour conditions. Eng Struct 2015;82:55–71. https://doi.org/10.1016/j. engstruct.2014.07.021.
- [53] Feng C-W, Ju S-H, Huang H-Y. Using a simple soil spring model and support vector machine to determine bridge scour depth and bridge safety. J Perform Constr Facil 2016;30. https://doi.org/10.1061/(ASCE)CF.1943-5509.0000837.
- [54] Zampieri P, Zanini MA, Faleschini F, Hofer L, Pellegrino C. Failure analysis of masonry arch bridges subject to local pier scour. Eng Fail Anal 2017;79:371–84. https://doi.org/10.1016/j.engfailanal.2017.05.028.
- [55] Mitoulis SA, Argyroudis SA, Loli M, Imam B. Restoration models for quantifying flood resilience of bridges. Eng Struct 2021;238:112180. https://doi.org/10.1016/ j.engstruct.2021.112180.
- [56] Argyroudis SA, Mitoulis SA. Vulnerability of bridges to individual and multiple hazards-floods and earthquakes. Reliab Eng Syst Saf 2021;210:107564. https:// doi.org/10.1016/j.ress.2021.107564.
- [57] Kallias AN, Imam B. Probabilistic assessment of local scour in bridge piers under changing environmental conditions. Struct Infrastruct Eng 2016;12:1228–41. https://doi.org/10.1080/15732479.2015.1102295.

- [58] Tubaldi E, Macorini L, Izzuddin BA, Manes C, Laio F. A framework for probabilistic assessment of clear-water scour around bridge piers. Struct Saf 2017;69:11–22. https://doi.org/10.1016/j.strusafe.2017.07.001.
- [59] Pizarro A, Manfreda S, Tubaldi E. The science behind scour at bridge foundations: a review. Water 2020;12:374. https://doi.org/10.3390/w12020374.
- [60] Lamb R, Aspinall W, Odbert H, Wagener T. Vulnerability of bridges to scour: insights from an international expert elicitation workshop. Nat Hazards Earth Syst Sci 2017;17:1393–409. https://doi.org/10.5194/nhess-17-1393-2017.
- [61] Maroni A, Tubaldi E, McDonald H, Zonta D. Monitoring-based adaptive water level thresholds for bridge scour risk management. Reliab Eng Syst Saf 2023;238: 109473. https://doi.org/10.1016/j.ress.2023.109473.
- [62] Carnacina I, Pagliara S, Leonardi N. Bridge pier scour under pressure flow conditions. River Res Appl 2019;35:844–54. https://doi.org/10.1002/rra.3451.
- [63] Kazantzi AK, Moutsianos S, Bakalis K, Mitoulis S-A. Cause-agnostic bridge damage state identification utilising machine learning. Eng Struct 2024;320:118887. https://doi.org/10.1016/j.engstruct.2024.118887.
- [64] Scozzese F, Ragni L, Tubaldi E, Gara F. Modal properties variation and collapse assessment of masonry arch bridges under scour action. Eng Struct 2019;199: 109665. https://doi.org/10.1016/j.engstruct.2019.109665.
- [65] Tubaldi E, White CJ, Patelli E, Mitoulis SA, de Almeida G, Brown J, et al. Invited perspectives: challenges and future directions in improving bridge flood resilience. Nat Hazards Earth Syst Sci 2022;22:795–812. https://doi.org/10.5194/nhess-22-795-2022.
- [66] CEN. EN 1991-1-6: Eurocode 1: actions on structures part 1-6: general actions actions during execution. [Authority: The European Union Per Regulation 305/ 2011, Directive 98/34/EC, Directive 2004/18/EC]: 2005.
- [67] Kazantzi AK, Righiniotis TD, Chryssanthopoulos MK. Fragility and hazard analysis of a welded steel moment resisting frame. J Earthq Eng 2008;12:596–615. https://doi.org/10.1080/13632460701512993.
- [68] Rossetto T, Ioannou I, Grant DN. Existing empirical vulnerability and fragility functions: compendium and guide for selection. GEM Technical Report 2015-1: 2015. https://doi.org/10.13117/GEM.VULN-MOD.TR2015.01.
- [69] Cornell CA, Jalayer F, Hamburger RO, Foutch D. Probabilistic basis for 2000 SAC federal emergency management agency steel moment frame guidelines. J Struct Eng 2002;128:526–33. https://doi.org/10.1061/(ASCE)0733-9445(2002)128:4 (526).
- [70] Bakalis K, Vamvatsikos D. Seismic fragility functions via nonlinear response history analysis. J Struct Eng 2018;144:04018181. https://doi.org/10.1061/(ASCE) ST.1943-541X.0002141.
- [71] Stefanidou S, Karatzetzou A, Tsinidis G, Mitoulis S, Argyroudis S. Multi-hazard fragility assessment of bridges: methodology and case study application. In: Proc., 3rd International Conference on Natural Hazards and Infrastructure, ICONHIC 2022: 2022.
- [72] Carozza S. Performance-based structural reliability assessment for rainfall-induced hydrogeological phenomena. PhD thesis. University of Naples Federico II, Department of Structures for Engineering and Architecture; 2017. https://doi.org/ 10.6093/UNINA/FEDOA/11462.
- [73] Kosić M, Anžlin A, Bau' V. Flood vulnerability study of a roadway bridge subjected to hydrodynamic actions, local scour and wood debris accumulation. Water 2022; 15:129. https://doi.org/10.3390/w15010129.
- [74] Mitoulis SA, Argyroudis SA, Loli M, Imam B. Restoration models for quantifying flood resilience of bridges. Eng Struct 2021;238:112180. https://doi.org/10.1016/ j.engstruct.2021.112180.
- [75] Kazantzi AK, Karaferis ND, Melissianos VE, Bakalis K, Vamvatsikos D. Seismic fragility assessment of building-type structures in oil refineries. Bull Earthq Eng 2022;20:6853–76. https://doi.org/10.1007/s10518-022-01476-y.
   [76] Tubaldi E, Antonopoulos C, Mitoulis SA, Argyroudis S, Gara F, Ragni L, et al. Field
- [76] Tubaidi E, Antonopoulos C, Mitoulis SA, Argyroudis S, Gara F, Kagni L, et al. Field tests and numerical analysis of the effects of scour on a full-scale soil-foundation-structural system. J Civ Struct Health Monit 2023;13:1461–81. https://doi.org/10.1007/s13349-022-00608-x.
- [77] Aygün B, Dueñas-Osorio L, Padgett JE, DesRoches R. Efficient longitudinal seismic fragility assessment of a multispan continuous steel bridge on liquefiable soils. J Bridge Eng 2011;16:93–107. https://doi.org/10.1061/(ASCE)BE.1943-5592.0000131.
- [78] Mckay MD, Beckman RJ, Conover WJ. A comparison of three methods for selecting values of input variables in the analysis of output from a computer code. Technometrics 2000;42:55–61. https://doi.org/10.1080/ 00401706.2000.10485979.
- [79] Ayyub BM, Mccuen RH. Simulation-based reliability methods. probabilistic structural mechanics handbook. Boston, MA: Springer US; 1995. p. 53–69. https://doi.org/10.1007/978-1-4615-1771-9 4.
- [80] Krawinkler H, Seneviratna GDPK. Pros and cons of a pushover analysis of seismic performance evaluation. Eng Struct 1998;20:452–64. https://doi.org/10.1016/ S0141-0296(97)00092-8.
- [81] Filizadeh R, Hernandez EM, Rosowsky DV. Risk-based framework for postearthquake monitoring and evaluation of reinforced concrete bridges subject to multiple hazards. Reliab Eng Syst Saf 2024;245:109992. https://doi.org/10.1016/ i.rosc.2024.100092
- [82] Scozzese F, Tubaldi E, Dall'Asta A. Damage metrics for masonry bridges under scour scenarios. Eng Struct 2023;296:116914. https://doi.org/10.1016/j. engstruct.2023.116914.
- [83] Guo X. Seismic vulnerability analysis of scoured bridge systems. PhD Thesis. University of Missouri-Kansas City; 2014. https://hdl.handle.net/10355/45577.
- [84] Kaya A. Artificial neural network study of observed pattern of scour depth around bridge piers. Comput Geotech 2010;37:413–8. https://doi.org/10.1016/j. compgeo.2009.10.003.

- [85] Pizarro A, Tubaldi E. Quantification of modelling uncertainties in bridge scour risk assessment under multiple flood events. Geosciences 2019;9:445. https://doi.org/ 10.3390/geosciences9100445.
- [86] Kosič M, Prendergast LJ, Anžlin A. Analysis of the response of a roadway bridge under extreme flooding-related events: scour and debris-loading. Eng Struct 2023; 279:115607. https://doi.org/10.1016/j.engstruct.2023.115607.
- [87] Martínez-Martínez LH, Delgado-Hernández DJ, De-León-Escobedo D, Flores-Gomora J, Arteaga-Arcos JC. Woody debris trapping phenomena evaluation in bridge piers: a Bayesian perspective. Reliab Eng Syst Saf 2017;161:38–52. https://doi.org/10.1016/j.ress.2017.01.005.
- [88] Chen X, Xiang N, Guan Z, Li J. Seismic vulnerability assessment of tall pier bridges under mainshock-aftershock-like earthquake sequences using vector-valued
- intensity measure. Eng Struct 2022;253:113732. https://doi.org/10.1016/j.engstruct.2021.113732.
- [89] Abdel-Mooty MN, Sasidharan M, Herrera M, Parlikad AK, Schooling J, El-Dakhakhni W, et al. Strategic assessment of bridge susceptibility to scour. Reliab Eng Syst Saf 2024;251:110334. https://doi.org/10.1016/j.ress.2024.110334.
- [90] Mühlhofer E, Koks EE, Kropf CM, Sansavini G, Bresch DN. A generalized natural hazard risk modelling framework for infrastructure failure cascades. Reliab Eng Syst Saf 2023;234:109194. https://doi.org/10.1016/j.ress.2023.109194.
- [91] Monti G, Demartino C, Gardoni P. Towards risk-targeted seismic hazard models for Europe. Sci Rep 2023;13:10717. https://doi.org/10.1038/s41598-023-36947-y.